

Supporting Information

Effects of the preparation method of Pt/g-C₃N₄ photocatalysts on efficiency for visible-light hydrogen production

Xuanbo Zhou, Yunfeng Li, Yan Xing,* Junsong Li, Xin Jiang

Experimental

Synthesis of bulk g-C₃N₄ and ultrathin porous g-C₃N₄ nanosheets

The bulk g-C₃N₄ powder was prepared by the thermal polycondensation of melamine according to a reported procedure.^[S1] In a typical process, 5 g of melamine was heated at 773 K for 2 h with a rate of 2 K min⁻¹ and then maintained at 793 K for another 2 h, followed by grinding the resultant yellow powder. Then, 1 g of the bulk g-C₃N₄ powder was further heated at 793 K in an alumina ark for several hours in an air atmosphere to obtain the final ultrathin porous g-C₃N₄ nanosheets.

Synthesis of Pt/g-C₃N₄ nanocomposites

The Pt/g-C₃N₄ nanocomposites were prepared by chemical reduction method. 15 mg of g-C₃N₄ nanosheets were added into 20 mL of distilled water in a 50 mL beaker and treated by sonication for 30 min. After this, 0.0294 g of trisodium citrate and a calculated amount of chloroplatinic acid (H₂PtCl₆·6H₂O) solution (0.038 M) were added to the above mixture under vigorous stirring for 1 h. Then, NaBH₄ aqueous solution (0.01M, 0.36 mL) was added into the mixture solution slowly as a reductant to reduce Pt. After stirring for 20 min, the samples were obtained by centrifuging and washed with distilled water for several times. The weight percentage ratios of Pt NPs to g-C₃N₄ nanosheets were 0, 1.0, 1.5, 2.0, and 2.5 wt%, which were labeled as CNS, 1.0%-Pt/CNS-CR, 1.5%-Pt/CNS-CR, 2.0%-Pt/CNS-CR and 2.5%-Pt/CNS-CR, respectively. The Pt/CNB-CR sample were also prepared by the same method except

using bulk g-C₃N₄ instead of ultrathin porous g-C₃N₄ nanosheets.

Meanwhile, 0.1 g of g-C₃N₄ nanosheets were dispersed in 30 mL of distilled water containing 2 wt% Pt-precursor (H₂PtCl₆·6H₂O) solution. Next, the mixture solution was irradiated by a 300 W Xenon lamp for 2 h to reduce H₂PtCl₆·6H₂O. After 2 h of photo-deposition, the sample was washed with distilled water and dried in oven. The as-obtained sample was denoted as 2.0%-Pt/CNS-PR. For comparison, the different loading amount of Pt for Pt/CNS-PR sample were prepared, which is labeled as 1.0%-Pt/CNS-PR, 1.5%-Pt/CNS-PR and 2.5%-Pt/CNS-PR, respectively. The actual loading amount of Pt NPs for all samples are listed in the Table S1.

Photocatalytic activity

The photocatalytic activity of samples for H₂ production was evaluated under visible light irradiation by a 300 W Xenon lamp equipped with a cutoff filter (≥ 420 nm). Typically, 10 mg of photocatalyst powder were added to 50 mL distilled water containing 6 mL TEOA as the sacrificial reagent and then illuminated with a 300 W Xenon lamp. The photocatalytic H₂ evolution rate was determined by a GC-7920 instrument with a thermal conductivity detector (TCD) and high-purity N₂ as the carrier gas.

Turnover frequency calculations

Turnover-Frequency (TOF) calculation in this paper uses the method reported by Yao et al. (ACS Appl. Mater. Inter. 2016, 8, 20667).

$$\text{TOF} = \frac{\text{moles of H}_2 \text{ molecules evolved}}{\text{moles of surface atoms of catalyst} \times \text{reaction time}}$$

(a) Mole of surface atoms of catalyst

Mole of surface atoms of Pt nanoparticles = (Number of Pt atoms on the surface of each Pt nanoparticles / number of Pt atoms in each Pt nanoparticles) \times mole of Pt nanoparticles

(b) Number of Pt atoms on the surface of each Pt nanoparticles

Number of Pt atoms on the surface of each Pt nanoparticles = (surface area of each nanoparticles / surface area of each two-dimensional unit cell on the {111} facets) × atoms in each two-dimensional unit cell on the {111} facets

(c) Number of Pt atoms in each Pt nanoparticles

Number of Pt atoms in each Pt nanoparticles = (volume of each nanoparticles / volume of each unit cell) × atoms in each unit cell

Characterization

The crystal phases were analyzed by X-ray powder diffraction on Siemens D5005 Diffractometer with Cu K α radiation ($\lambda = 1.5418 \text{ \AA}$). Transmission electron microscopy (TEM) and high-resolution transmission electron microscopy (HRTEM) were conducted on JEM-2100F microscope. Scanning electron microscopy (SEM) images were obtained by using an XL30 ESEM FEG microscope. X-ray photoelectron spectroscopy (XPS) was analyzed on a Thermo ESCALAB 250 XPS instrument. Brunauer–Emmett–Teller (BET) surface area of the samples were measured on a Micromeritics Tristar 3000 analyzer at 77.4 K. The loadings of Pt were measured on inductively coupled plasma-atomic emission spectrometer (ICP-AES) on Prodigy 7. Photoluminescence (PL) spectra were measured by using a FLSP920 Edinburgh Fluorescence Spectrometer. UV-vis diffuse reflectance spectra (UV-vis DRS) were performed by using Cary 7000 spectrometer. Electrochemical analyses were performed on an electrochemical workstation (CHI660E, China) and the electrolyte was 0.1 M Na₂SO₄ solution.

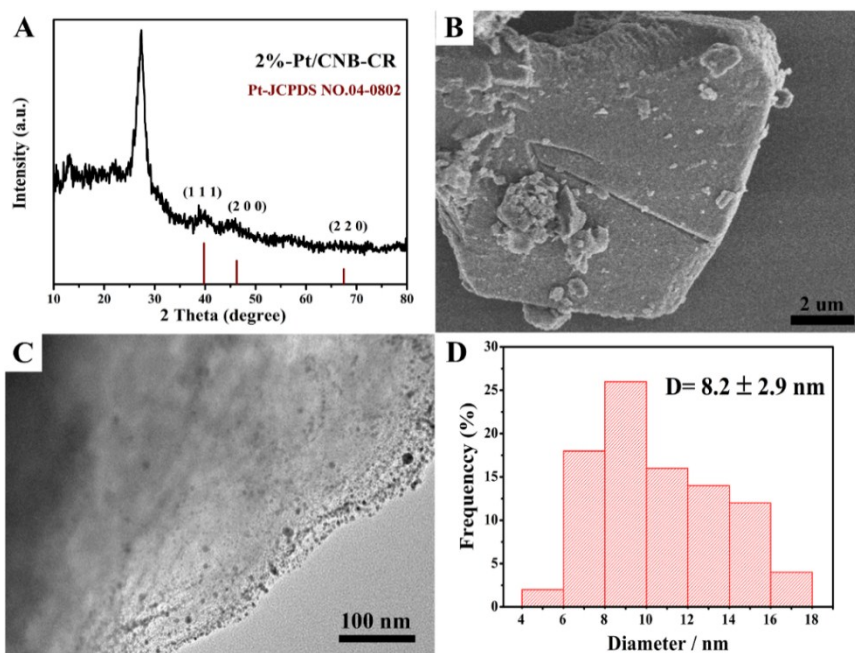


Figure S1. (A) XRD pattern of the 2.0%-Pt/CNB-CR nanocomposite. (B) SEM image of the pure CNB sample. (C) TEM image of the 2.0%-Pt/CNB-CR nanocomposite. (D) Size distribution histograms of Pt NPs in the 2.0%-Pt/CNB-CR nanocomposite.

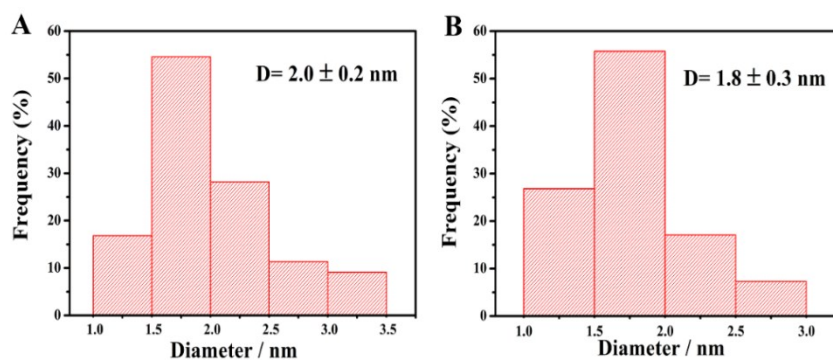


Figure S2. Size distribution histograms of Pt NPs (A) 2.0%-Pt/CNS-CR and (B) 2.0%-Pt/CNS-PR.

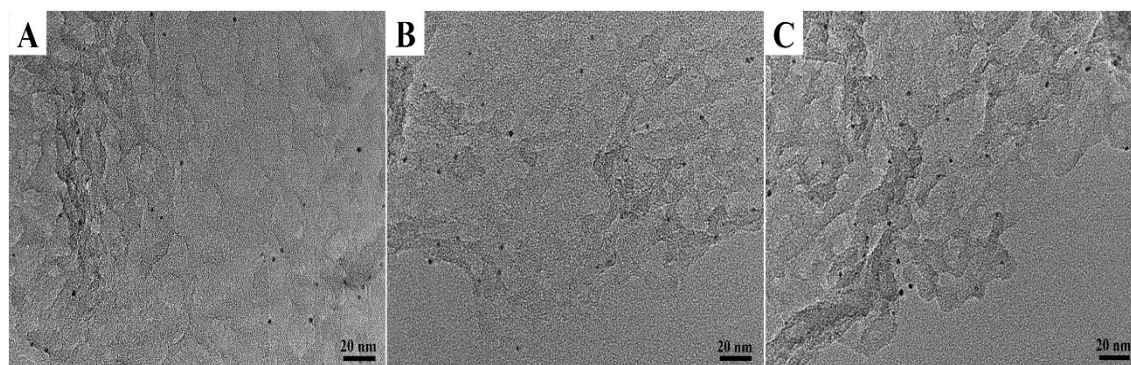


Figure S3. TEM images of (A) 1.0%-Pt/CNS-CR, (B) 1.5%-Pt/CNS-CR and (C) 2.5%-Pt/CNS-CR nanocomposites.

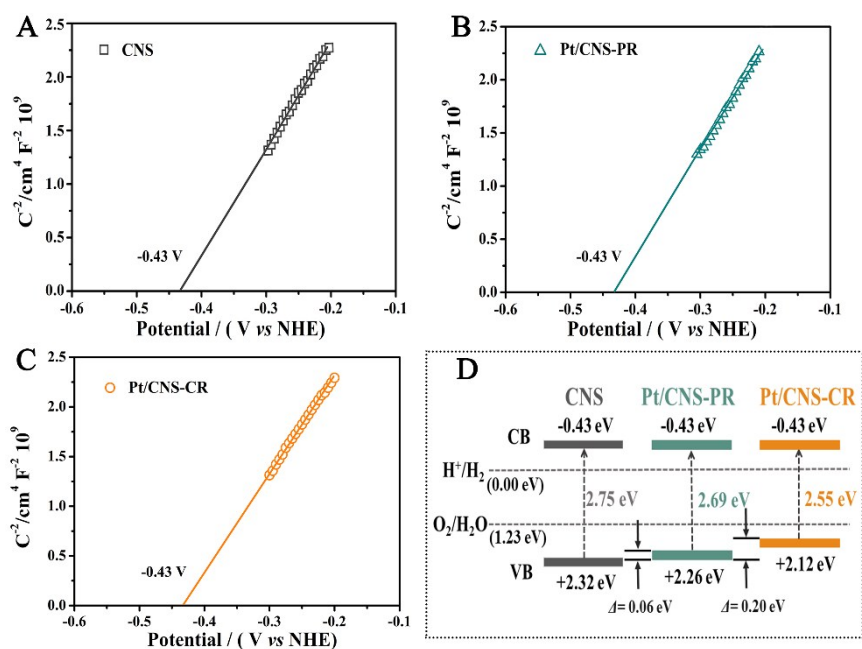


Figure S4. Mott-Schottky plots of (A) CNS, (B) 2.0%-Pt/CNS-PR and (C) 2.0%-Pt/CNS-CR samples. (D) Bandgap structures of CNS, 2.0%-Pt/CNS-PR and 2.0%-Pt/CNS-CR samples.

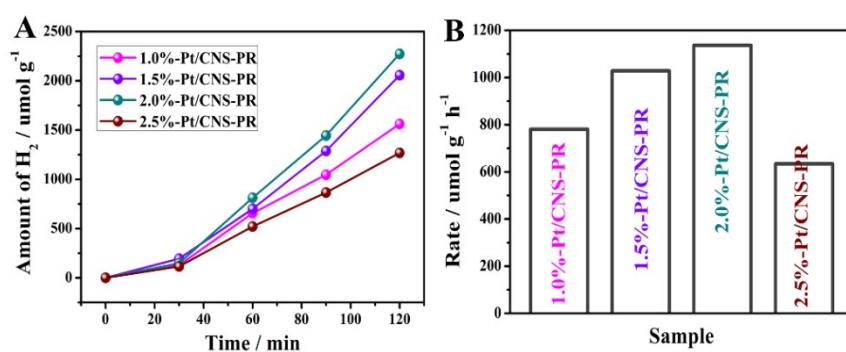


Figure S5. (A) Amount of H₂ generation and (B) Hydrogen evolution rate of the 1.0%-Pt/CNS-PR, 1.5%-Pt/CNS-PR, 2.0%-Pt/CNS-PR and 2.5%-Pt/CNS-PR samples.

Table S1. ICP analysis for the Pt/CNS-CR, Pt/CNS-PR and Pt/CNB-CR samples.

| Entry | Samples | The loading amount of Pt (wt%) |
|-------|----------------|--------------------------------|
| 1 | 1.0%-Pt/CNS-CR | 0.85 |
| 2 | 1.5%-Pt/CNS-CR | 1.11 |
| 3 | 2.0%-Pt/CNS-CR | 1.60 |
| 4 | 2.5%-Pt/CNS-CR | 1.84 |
| 5 | 2.6%-Pt/CNS-CR | 1.90 |
| 6 | 1.0%-Pt/CNS-PR | 0.88 |
| 7 | 1.5%-Pt/CNS-PR | 1.36 |
| 8 | 2.0%-Pt/CNS-PR | 1.90 |
| 9 | 2.5%-Pt/CNS-PR | 2.30 |
| 10 | 2.0%-Pt/CNB-CR | 1.92 |

Table S2. Comparison of the hydrogen production rates over noble metal modified g-C₃N₄ based photocatalysts reported in the literature with that of the present study.

| Photocatalyst | Sacrificial reagents | Light source | H₂ evolution (μmol g⁻¹ h⁻¹) | Ref. |
|--|-----------------------------|------------------------------|---|-------------|
| Ag@C ₃ N ₄ | triethanolamine | λ > 420 nm | 25.2 | S2 |
| Pt-g-C ₃ N ₄ | oxalic acid | λ ≥ 420 nm | 3900 | S3 |
| Pt/g-C ₃ N ₄ | triethanolamine | λ ≥ 400 nm | 588 | S4 |
| Pt/g-C ₃ N ₄ -P-OH | triethanolamine | λ ≥ 420 nm | 400 | S5 |
| Pt/g-C ₃ N ₄ | triethanolamine | λ > 420 nm | 97.5 | S6 |
| Pd-Ag/g-C ₃ N ₄ | triethanolamine | solar light | 1250 | S7 |
| Pt-g-C ₃ N ₄ | triethanolamine | λ = 520 nm | 3420 | S8 |
| AuPd/g-C ₃ N ₄ | triethanolamine | λ ≥ 400 nm | 326 | S9 |
| Pt/pm-g-C ₃ N ₄ | triethanolamine | λ ≥ 420 nm | 417 | S10 |
| CNS-Pt-A | triethanolamine | without adding cutoff filter | 972.2 | S11 |
| Ag/g-C ₃ N ₄ | triethanolamine | without adding cutoff filter | 2014.20 | S12 |
| Pd/2D-C ₃ N ₄ | triethanolamine | λ > 400 nm | 1208.6 | S13 |
| 2.0%-Pt/CNS-CR | triethanolamine | λ ≥ 420 nm | 7862.5 | This work |

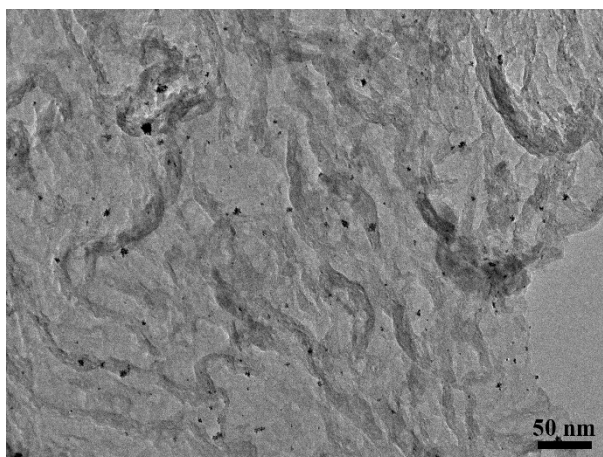


Figure S6. TEM image of the 2.0%-Pt/CNS-CR nanocomposite after 10 cycles of the photocatalytic hydrogen production reaction.

Notes and References

- S1 Y. F. Li, R. X. Jin, X. Fang, Y. Yang, M. Yang, X. C. Liu, Y. Xing and S. Y. Song, *J. Hazard. Mater.*, 2016, **313**, 219.
- S2 X. J. Bai, R. L. Zong, C. X. Li, D. Liu, Y. F. Liu and Y. F. Zhu, *Appl. Catal., B*, 2014, **147**, 82.
- S3 F. Fina, H. Ménard and J. T. S. Irvine, *Phys. Chem. Chem. Phys.*, 2015, **17**, 13929.
- S4 S. W. Cao, J. Jiang, B. C. Zhu and J. G. Yu, *Phys. Chem. Chem. Phys.*, 2016, **18**, 19457.
- S5 Z. H. Wang, X. F. Peng, S. S. Tian and Z. Wang, *Mater. Res. Bull.*, 2018, **104**, 1.
- S6 Y. Shiraishi, Y. Kofuji, S. Kanazawa, H. Sakamoto, S. Ichikawa, S. Tanaka and T. Hirai, *Chem. Commun.*, 2014, **50**, 15255.
- S7 I. Majeed, U. Manzoor, F. K. Kanodarwala, M. A. Nadeem, E. Hussain, H. Ali, A. Badshah, J. A. Stride and M. A. Nadeem, *Catal. Sci. Technol.*, 2018, **8**, 1183.
- S8 Y. Xue, Y. G. Lei, X. Y. Liu, Y. N. Li, W. A. Deng, F. Wang and S. X. Min, *New J. Chem.*, 2018, **42**, 14083.
- S9 C. C. Han, L. E. Wu, L. Ge, Y. J. Li and Z. Zhao, *Carbon*, 2015, **92**, 31.
- S10 Y. J. Zhong, Z. Q. Wang, J. Y. Feng, S. C. Yan, H. T. Zhang, Z. S. Li and Z. G. Zou, *Appl. Surf. Sci.*, 2014, **295**, 253.
- S11 M. J. Liu, P. F. Xia, L. Y. Zhang, B. Cheng and J. G. Yu, *ACS Sustainable Chem. Eng.*, 2018, **6**, 10472.

S12 J. Y. Qin, J. P. Huo, P. Y. Zhang, J. Zeng, T. T. Wang and H. P. Zeng, *Nanoscale*, 2016, **8**, 2249.

S13 Z. Mo, H. Xu, X. J. She, Y. H. Song, P. C. Yan, J. J. Yi, X. W. Zhu, Y. C. Lei, S. Q. Yuan and H. M. Li, *Appl. Surf. Sci.*, 2019, **467**, 151.